CHAPTER 4

RESULTS AND DISCUSSION - PART 1: OPTIMIZED PROCESSING CONDITION FOR PZT AND PZT-BASED NANOCOMPOSITE THIN FILMS

In this chapter, the results of PZT thin film synthesis are analyzed to find the optimized processing condition for PZT thin film preparation. Effects of heating condition and Pb excess on phase and dielectric properties of the films were investigated to figure out the optimized condition for preparation of high quality films. The optimized condition was also used to prepare PZT-based nanocomposite films (PZT/WO_3 and PZT/CuO). At the first stage, the heating steps of PZT/WO_3 film were studied to examine microstructure, and acquire dense and crack-free films.

4.1 PZT thin film

There is a great potential for exploiting the ferroelectric, pyroelectric and piezoelectric properties of PZT thin films as memory, imaging and electromechanical devices, etc. Sol–gel coating techniques have been a popular means of fabricating films of perovskite compositions in the submicrometer thickness range [111]. The techniques involve the deposition of amorphous gel film which is subsequently transformed to a crystalline phase during annealing process. However, resultant phases, microstructure, texture and electrical properties of the films depend on various parameters, including film composition, heating rate, drying condition and annealing temperature. In previous work, thermal processing parameter was one of the main factors in which affected crystallization behavior of perovskite thin films [119]. This research thus aims to study a preparation procedure of crystalline PZT thin films with a composition $Pb(Zr_{0.52}Ti_{0.48})0_3$ using sol-gel and spin coating techniques. In this chapter, the effects of heating cycle and excess Pb content on phase and microstructures are determined.

4.1.1 Differential thermal analysis and thermogravimetric analysis

The results of thermal analysis (DTA) on PZT gel is shown in Fig. 1. The DTA line shows both endothermic and exothermic peaks, and the thermogravimetric (TG) line shows mass losses as a function of annealing temperature. The endothermic peak at 80°C and the initial 2% mass loss together represented the evaporation of residual absorbed alcohol and water [120]. The 10% mass loss was accompanied by the exothermic peak at 300°C. This exothermic peak was found to be associated with the chelated acetylacetone PZT sol–gel route and identified to be the decompositional product of acetate groups [121]. Two consecutive endothermic peaks at 340°C and 390°C were associated with the organic decomposition [122], which altered the amount of weight loss substantially. Approximately 10% of weight loss occurred as temperature increased from 390°C to 500°C, and the weight loss leveled off at around 570°C. These changes suggested that, for the preparation of PZT, PZT/WO_3 and PZT/CuO films, the annealing temperature of 600°C was sufficient to obtain the complete perovskite phase.

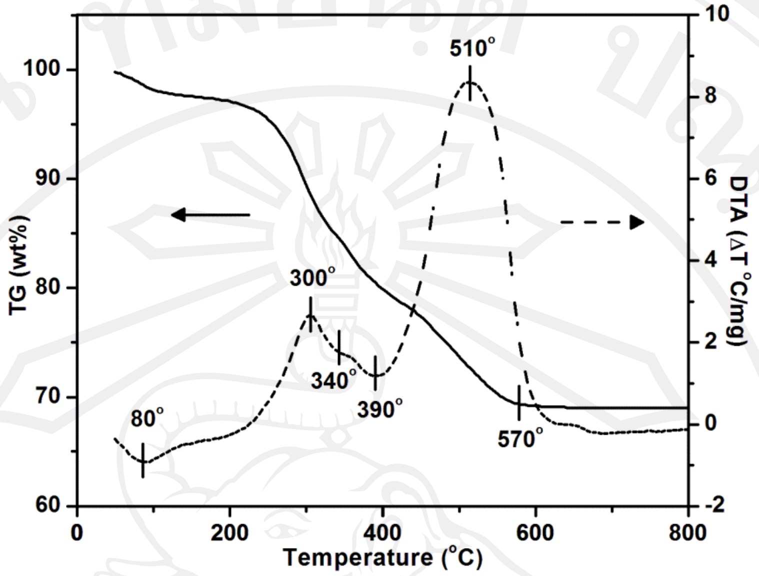

Figure 4.1 TG/DTA graphs of PZT sol-gel powder.

4.1.2 X-ray diffraction pattern analysis

4.1.2.1 Effect of annealing temperature on phase of PZT thin films

Phase characteristics of a series of heat-treated PZT films (thickness ~ 400 nm) are shown in Fig. 4.2 and 4.3. The X-ray diffraction patterns in Fig. 4.2 shows the patterns of (a) Pt/Ti/SiO_2/Si substrate and (b) unheated PZT solution on substrate which was dried at room temperature. The substrate shows platinum (Pt) and silicon (Si) phases. When PZT solution was deposited on the substrate without heating and drying at room temperature, a broad amorphous peak of the unheated PZT solution at 2θ about 29° was observed (Fig. 4.2(b)).

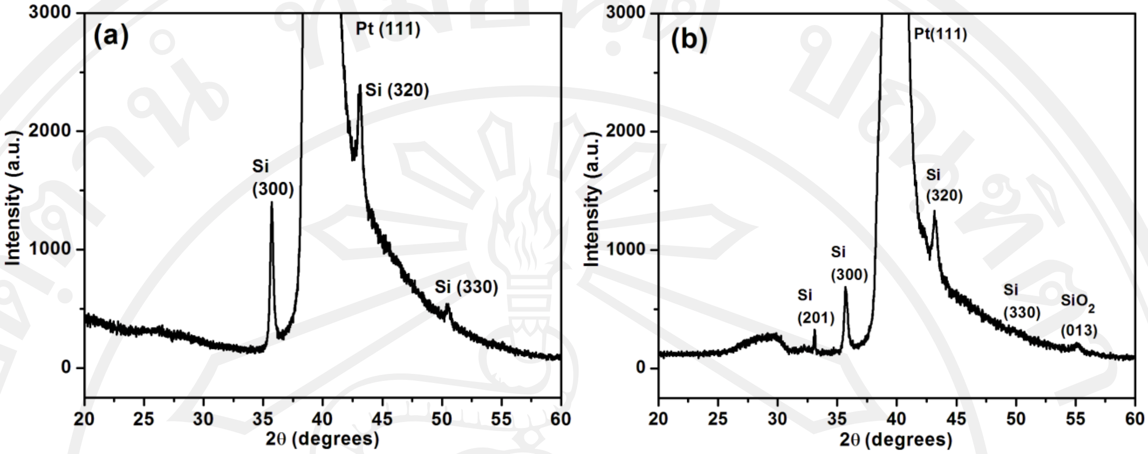

Figure 4.2 XRD pattern of (a) substrate and (b) PZT solution deposited on a substrate without heat treatment.

After heat treatment, the X-ray diffraction patterns are shown in Fig. 4.3, which shows phase evolution of PZT thin films with annealing temperature. The heat treatment temperatures at (a) 200°C and (b) 300°C exhibited the substrate peaks and a broad peak at about $2\theta \approx 29°$ which could be an uncompleted reaction (intermediate phase) of PZT perovskite. When increasing the heat treatment temperature to 400°C, the $PbPt_x$, Pt, Si, SiO_2 and together with an intermediate phase of PZT ($2\theta \approx 29°$) were detected. However, the $PbPt_x$ phase indicated the diffusion between PZT layer and Pt electrode (Fig. 4.3(c)) [123, 124]. With further increase in the heat treatment temperature to 500°C, the crystalline perovskite phase of PZT appeared.

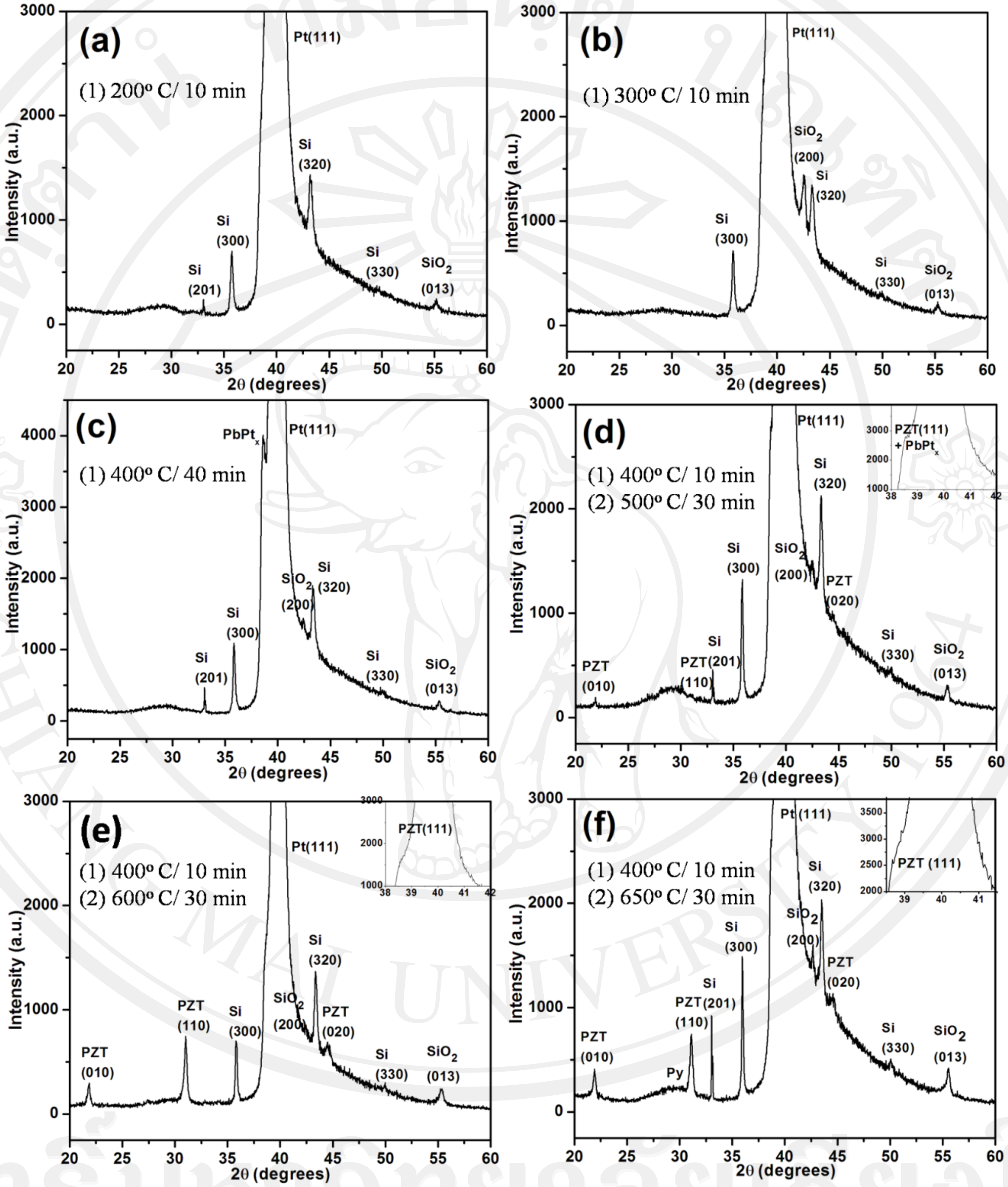

Figure 4.3 XRD patterns of PZT thin films with various heat treatment conditions: (1) is a pre-heating temperature and (2) is an annealing temperature.

However, the peak at 2θ ≈ 39° is $PbPt_x$ phase mixed with PZT (111). This peak included an intermediate phase of PZT at 2θ which is about 29° as shown in Fig. 4.3(d). Thus, the film became a fully crystallized perovskite phase without secondary phases when the films were annealed at 600°C as shown in Fig. 4.3(e). Nevertheless, a broad peak at 2θ = 29° which belongs to pyrochlore phase (P_y) appeared at a higher annealing temperature (650°C) as shown in Fig. 4.3(f).

Such results are expected to be due to Pb loss at high annealing temperatures. The orientation analysis was conducted through a measurement of PZT peak intensity ratio of the PZT thin films (Table 4.1). However, PZT perovskite phase was not present in the films annealed up to 400°C. Thus, the low intensity (010) and (110) PZT reflections appeared when increasing annealing temperature over 500°C. It was found that when annealing temperatures were increased, the (111) and (110) PZT intensities decreased while (010) PZT intensity increased as listed in Table 4.1. This indicated that Pb loss at high annealing temperatures affected on the growth direction of PZT thin films [119]. In this work, PZT films were annealed at 600°C, and the films showed the best crystallization of perovskite phase compared to the other annealing temperatures.

Table 4.1 Percentages of the PZT peak intensity ratio as a function of annealing temperature.

The orientation of PZT (%)	Annealing temperature (°C)	
	600	650
111	62.21	62.03
110	27.04	17.69
010	10.74	12.16
Pyrochlore	0	8.11

Note : The orientation ratios were calculated according to (010): $I_{(010)}/[I_{(010)}+I_{(110)}+I_{(111)}+I_{(Py)}]$, (110) :$\mathrm{I}_{(110)}/[\mathrm{I}_{(010)}+\mathrm{I}_{(110)}+\mathrm{I}_{(111)}+\mathrm{I}_{(Py)}]$, (111): $I_{(111)}/[I_{(010)}+I_{(110)}+I_{(111)}+I_{(Py)}]$, and (Pyrochlore) : $I_{(Py)}/[I_{(010)}+I_{(110)}+I_{(111)}+I_{(Py)}]$.

4.1.1.2 Effect of excess Pb addition on phase of PZT thin films

It is well known that Pb in PZT system easily volatilizes during crystallization treatment, and some of excess Pb is adopted purposely to compensate for the volatilization. Thus, the effect of excess Pb addition on phase and orientation is a very important factor to grasp for a preparation of quality films because the electrical properties of ferroelectric films depend significantly on the phases and orientation [125]. The above effect was investigated at a heat-treated condition of 400 °C for 10 min and then annealed at 600 °C for 30 min. XRD patterns of PZT thin films with various contents of excess Pb (0-15 mol%) are shown in Fig. 4.4. All PZT films were crystallized into perovskite phase, with some differences in their preferred orientation. The presence of perovskite PZT (010), (110) and (111) peaks was observed for all compositions.

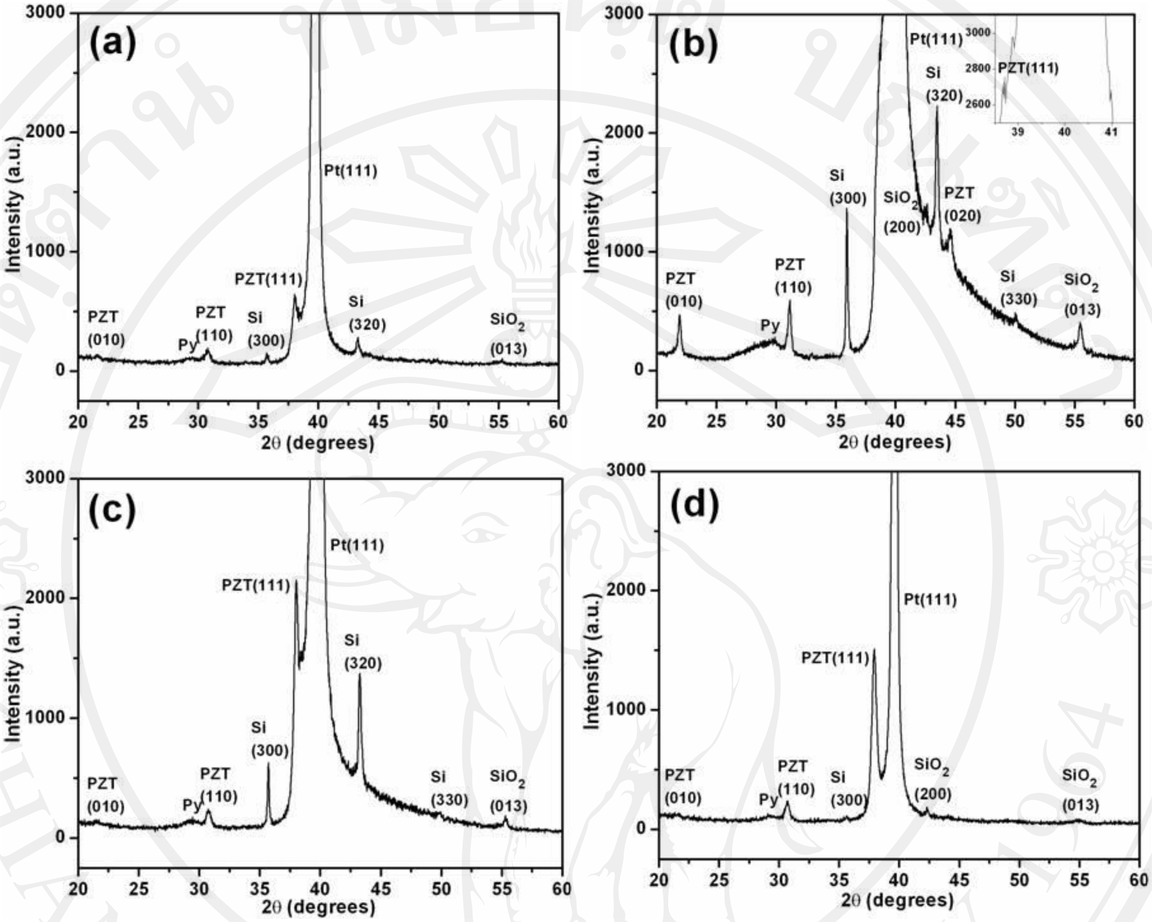

Figure 4.4 Comparison of XRD patterns of PZT thin films heat-treated at 400°C for 10 min and then annealed 600°C for 30 min at various contents of excess Pb: (a) 0 wt%, (b) 5 wt%, (c) 10 wt% and (d) 15 wt%.

Along with the increase in Pb concentration, the preferred orientation of PZT films changed from (010) and (110) to (111). It was found that the excess Pb enhanced the formation of Pb-Pt intermatallic phase which is easily formed and enhanced (111) oriented film [126]. The intermediate phases played an important role as nucleation sites for PZT thin films while transitioning phase from amorphous to perovskite phase [127, 128]. The orientation analysis graph of PZT thin films (percentages of the PZT peak intensity ratio on excess Pb addition) is shown in Fig. 4.5. The result indicated that a pyrochlore phase was also present in all compositions. The intensity of pyrochlore peak tended to decrease with the increase of excess Pb. Due to an ability to control Pb valence state, this effective composition control enabled a preparation of PZT films with less residual pyrochlore [119].

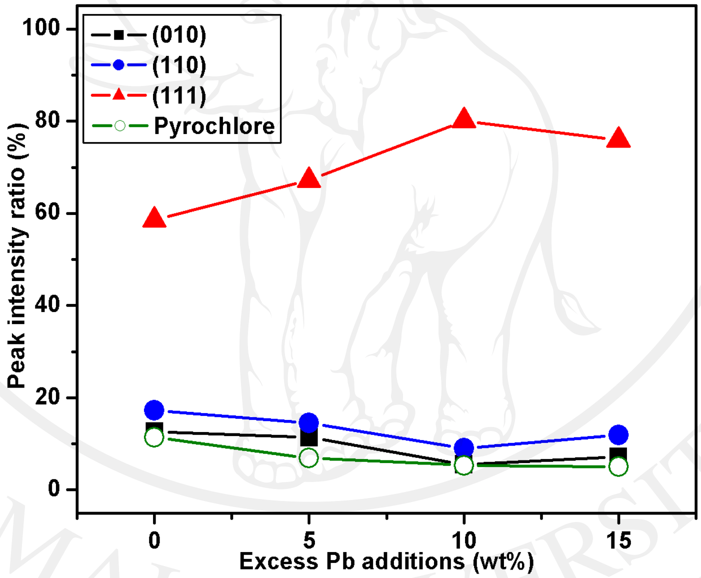

Figure 4.5 Percentages of the PZT peak intensity ratio as a function of excess Pb concentration. The peak intensity ratios were calculated according to (010): $I_{(010)}/[I_{(010)}+I_{(110)}+I_{(111)}+I_{(Py)}]$, (110): $I_{(110)}/[I_{(010)}+I_{(110)}+I_{(111)}+I_{(Py)}]$, (111): $I_{(111)}/[I_{(010)}+I_{(110)}+I_{(111)}+I_{(Py)}]$, and (Pyrochlore) : $I_{(Py)}/[I_{(010)}+I_{(110)}+I_{(111)}+I_{(Py)}]$.

Moreover, the study on dielectric properties of PZT thin films with varying excess Pb concentration have confirmed that the dielectric constants tended to increase with increasing Pb concentration (Table 4.2). In addition, the ferroelectric property also showed the same trend as shown in Fig 4.6. This phenomenon could be responsible by the prohibition of Pb loss in a heat treatment process as found earlier that the pyrochlore phase appeared at higher annealing temperatures. Also, the amount of pyrochlore phase decreased with increasing Pb-excess content. Furthermore, the lack of accurate chemical control in Pb-based system during heat treatment process could cause PbO loss and result in the formation of lead and oxygen vacancies [126, 129] as shown in equation (4.1). The vacancy can segregate to the domain walls and pin the domain walls movement [35]. This vacancy degraded both dielectric and ferroelectric properties of PZT thin films. For the 15 wt% excess Pb film, the dielectric and ferroelectric properties significantly dropped once again. This could be a result of the film's orientations. It was found that PZT(111) orientation was increased with increasing Pb concentration (0-10 wt%) but when Pb concentration was increased up to 15 wt%, the PZT(111) orientation fraction was reduced (Fig. 4.5). The PZT(111) orientation was reported to have good ferroelectric and dielectric properties [126]. Therefore, this could affect a reduction of the dielectric and ferroelectric properties in the film with 15 wt% excess of Pb. This implied that a variation in composition depending on the Pb content affected structure and electrical properties of PZT thin film. Thus, a condition of 10 wt% excess Pb and annealing temperature at 600°C was used for further study.

$$Pb_{Pb^x} + O_{(g)} \rightarrow PbO + V_{Pb}^{''} + V_O^{\cdot\cdot} \qquad (4.1)$$

Table 4.2 Dielectric properties as a function of excess Pb addition to PZT thin films

Dielectric properties (at RT)	Excess Pb addition (wt%)			
	0	5	10	15
ε_r	204	225	593	249
tanδ	0.12	0.07	0.09	0.26

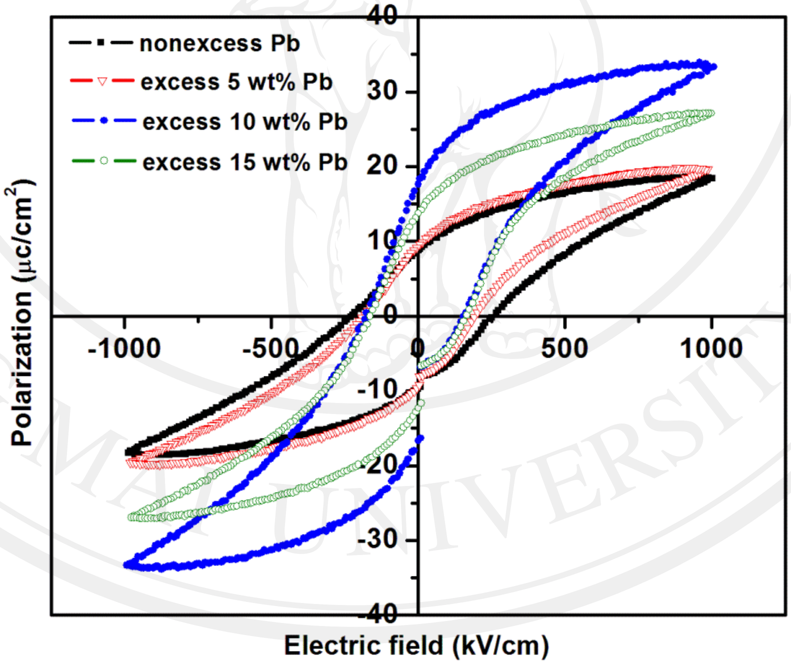

Figure 4.6 P-E hysteresis loops of PZT thin films with various concentrations of excess Pb.

4.1.3 Effect of heating step on microstructure of PZT thin films

Microstructures of PZT thin films prepared by varying heating steps are given in Fig. 4.7. Two types of cracks morphologies were observed in the dried films, i.e. a straight-type crack throughout the surface of the films and a random crazed-type crack on the edges of the films (Fig 4.8 conditions 1 and 2). The crazed-type cracks were generally observed in the films when the heating rate was abruptly changed. The occurrence of this type of crack was likely due to residual stresses in substrate or stress resulting from the shrinkage of gel layers [1]. On the other hand, the straight-type cracks presented throughout the film surface were also observed when the heating steps started at low temperature (Fig. 4.8 conditions 1 and 3). This is believed to be caused by organic or inorganic binders at the bottom of films could not easily evaporate due to the formation of a gel on the film surface. As a result, the pressure of binder expansion due to higher temperature created straight-type cracks. The formation of two types of cracks suggests that different mechanisms were operating under varying gelation and drying conditions. For this work, pre-heat temperature started at 400°C for 10 min by a custom-built hotplate and then annealed at 600°C for 30 min (condition 2) due to no crack observed in the films. However, the random crazed-type cracks still appeared at the edges of the films. The results showed that uncracked film could be achieved for the condition 4, but there was high content of bubbles inside the film. Accordingly, the densely crack-free film synthesized using condition 2 was selected for a preparation of PZT thin films, without a consideration of the cracked edges.

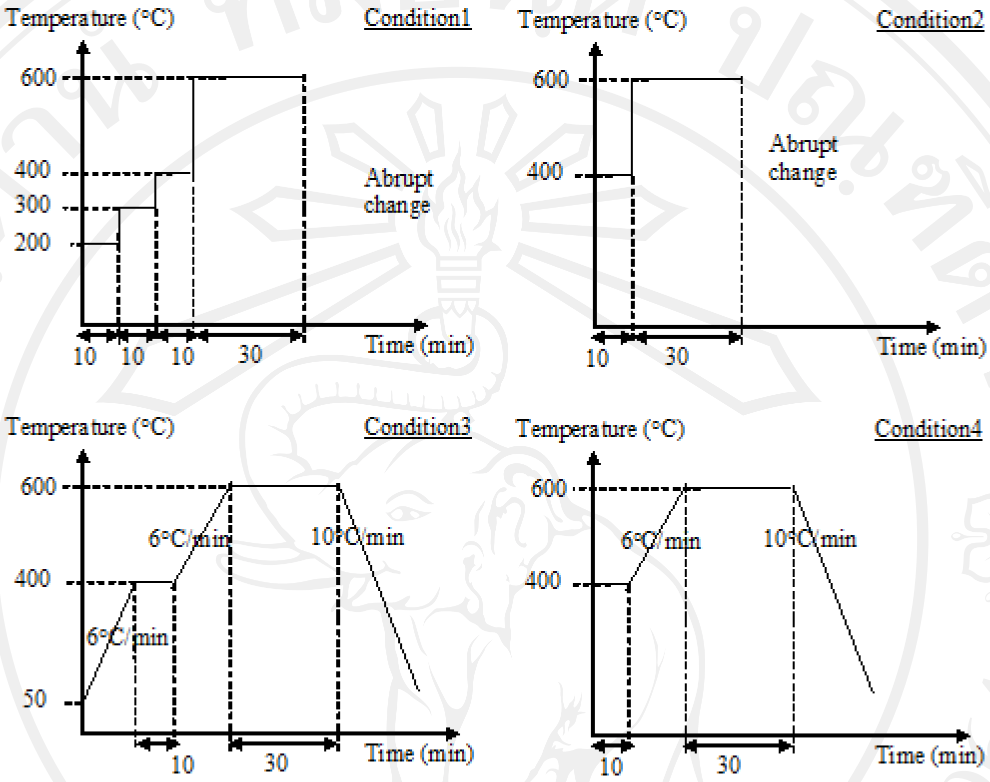

Figure 4.7 Various heating steps for studying of microstructure of PZT thin films.

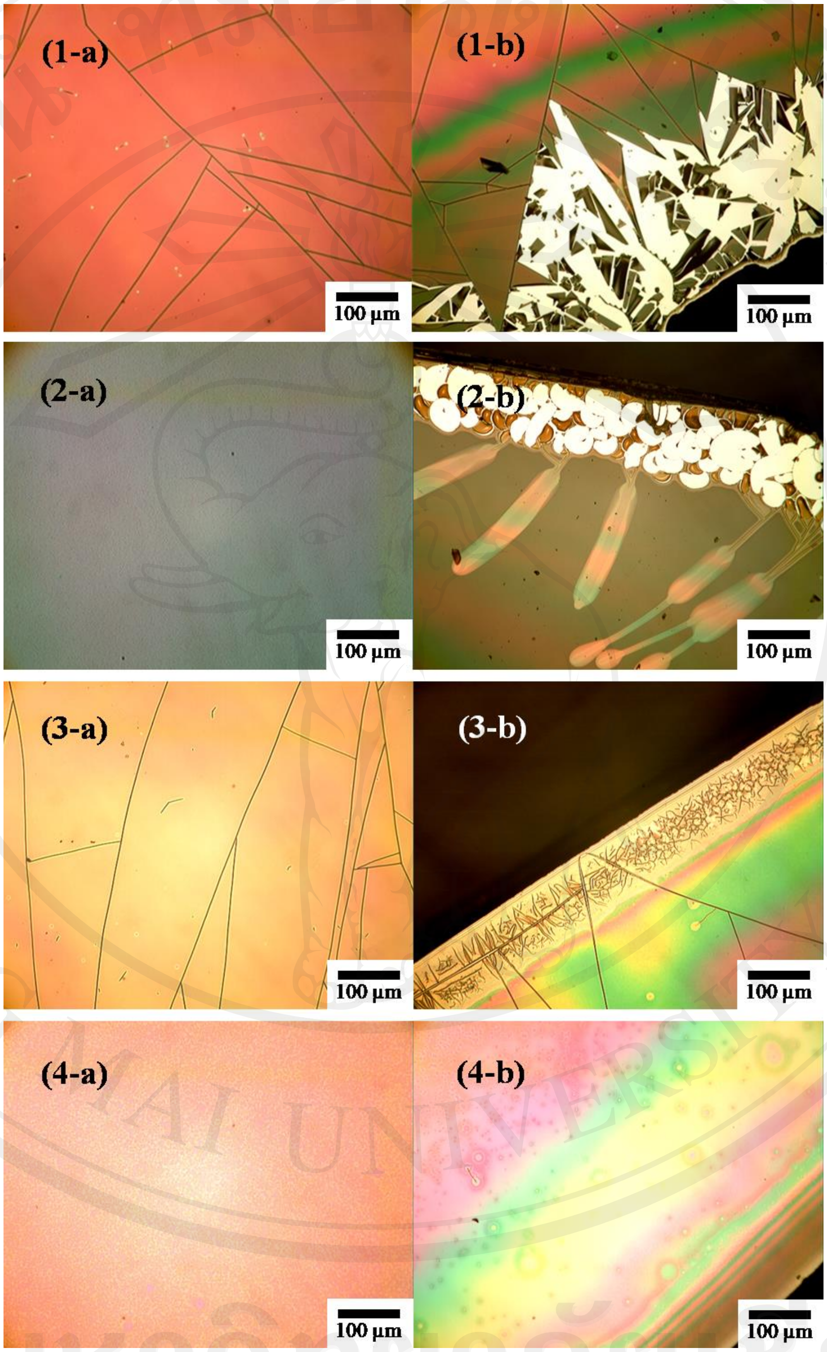

Figure 4.8 Optical micrographs of PZT thin films prepared by different heating steps, i.e. condition (1-4), see Fig. 4.7 for processing details, and (a-b) are film and film's edge, respectively.

4.2 PZT-based nanocomposite thin films

For preparation of PZT nanocomposite thin films, WO_3 and CuO nanoparticles are added into PZT-based thin film composites by dispersing nanoparticles into PZT sol and then spin-coating on platinized silicon substrate. In this section, preliminary work on the effects of WO_3 nanoparticles on the phase and microstructure of PZT thin films are investigated and discussed.

4.2.1 Microstructure of PZT/WO_3 nanocomposite thin films

In order to study the microstructure of PZT-based nanocomposite thin films, the optimum processing conditions included excess lead, annealing temperature and heating step for preparation of pure PZT thin film revealed by the preliminary studies were used. The films were prepared by 10 wt% excess Pb with WO_3 nanoparticle which dispersed in PZT solution and spin-coated onto a substrate. The film was then pre-heated on a hot-plate at 400°C for 10 min and annealed at 600°C for 30 min. However, the crack still appeared in the film as shown in Table 4.3 (condition 1). Therefore, the optimum heating condition needed to be revealed to prepare a better quality film. To achieve this, the heat treatment temperature was fixed at 400°C for 10 min for pre-heating temperature. The annealing temperature of 600°C for 30 min was used due to the high amount of perovskite phase could be obtained as found in the previous study.

Microstructures of PZT thin films prepared by varying heating steps are given in Table. 4.3. All thin films fabricated at various conditions had shorter cracks which generally started to propagate from WO_3 nanoparticles, except for the films prepared using the condition 7. In condition 1, a layer of PZT/WO_3 film was deposited on the (111) preferred orientation of $Pt/Ti/SiO_2/Si$ substrate. This film contained cracks which stretched out of WO_3 particles. It was possible that the nanoparticles stood as an obstacle for the film shrinkage, and the thickness of the films may be too thin to cover the particles dispesed in the films. Apart from this, the lattices between PZT film and the nanoparticles did not well match, resulting short cracks due to the thermal expansion mismatch of both phases (see the detail in appendix). Accordingly, another layer of PZT/WO_3 film was deposited on the first layer, and a variety of heating steps were employed to study the microstructure of the films as shown in Table 4.3, i.e. condition 2-5. All of them still showed cracked films. The thicker films still could not get rid of the cracks in the composite films. However, the comparison of 1st and 2nd layers films as shown in the conditions 1 and 5 revealed that crack concentration of the 2nd layers film was reduced. This suggested that the film thickness more or less had some influences on a quality of the composite films. Thus, an additional layer of PZT solution (without WO_3) was deposited onto the PZT/WO_3 films. The pure PZT precursor solution was expected to infiltrate into pores (or defects) in the composite films to increase the film density as previously reported by Zhao [130]. The different heating steps were studied to acquire a better quality film. It was found that the film had a straight crack all over the film when the heating rate was abruptly changed as shown in the condition 2 and 6. It is considered to be a result of an abrupt change in temperature which caused high stress level and increased thermal expansion mismatch between PZT and WO_3 in the films.

Table 4.3 Optical micrographs of PZT/WO_3 nanocomposite thin films prepared with different processing conditions as shown in Table 3.3.

Condition	Film layer	Microstructure of films surface
1	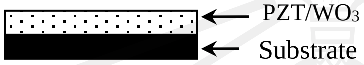 1) 400°C for 10 min then increased to 600°C with rate 6°C/min and leave for 30 min then cool down to room temperature; rate 10°C/min	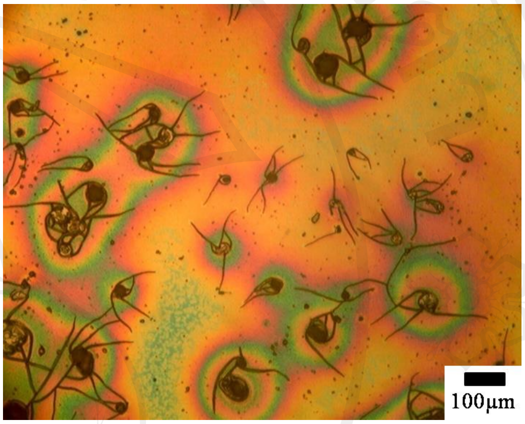
2	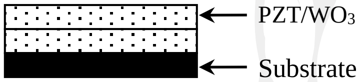 1) 400°C for 10 min 2) 400°C for 10 min then 600°C for 30 min	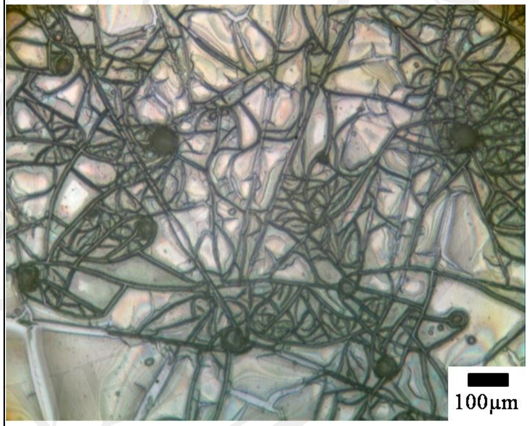
3	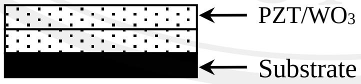 1) 400°C for 10 min 2) 400°C for 10 min then increased to 600°C with rate 6°C/min and leave for 30 min then cool down to room temperature; rate 10°C/min	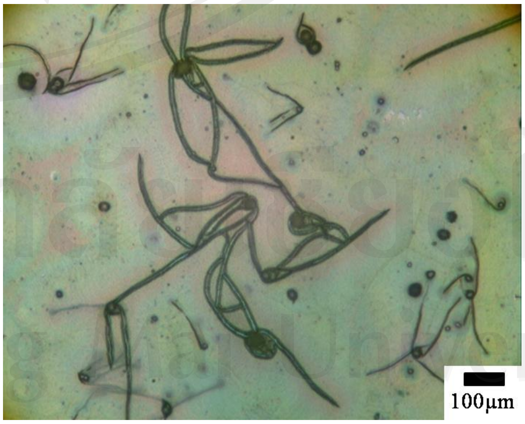

* 1) and 2) are heating condition for 1st and 2nd layers, respectively

Table 4.3 Optical micrographs of PZT/WO$_3$ nanocomposite thin films prepared with different processing conditions as shown in Table 3.3 (continue).

Condition	Film layer	Microstructure of films surface
4	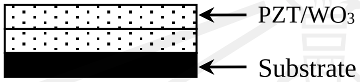 1) 400°C for 10 min then cool down to room temperature; rate 10°C/min 2) 400°C for 10 min then increased to 600°C with rate 6°C/min and leave for 30 min then cool down to room temperature; rate 10°C/min	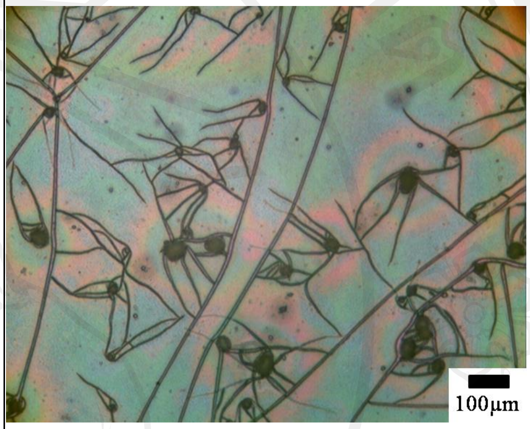
5	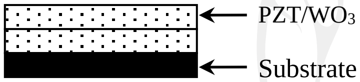 1) no heat 2) 400°C for 10 min then increased to 600°C with rate 6°C/min and leave for 30 min then cool down to room temperature; rate 10°C/min	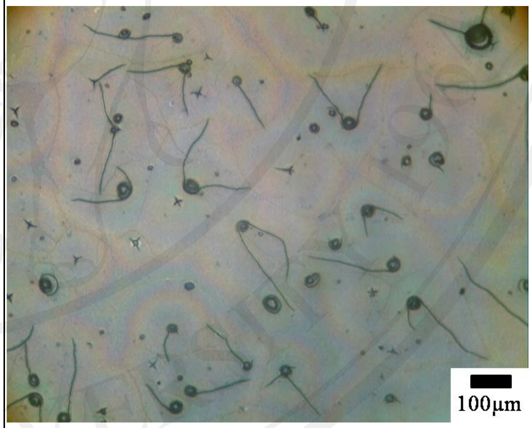
6	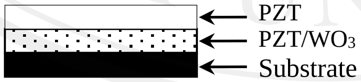 1) 400°C for 10 min 2) 400°C for 10 min then 600°C for 30 min	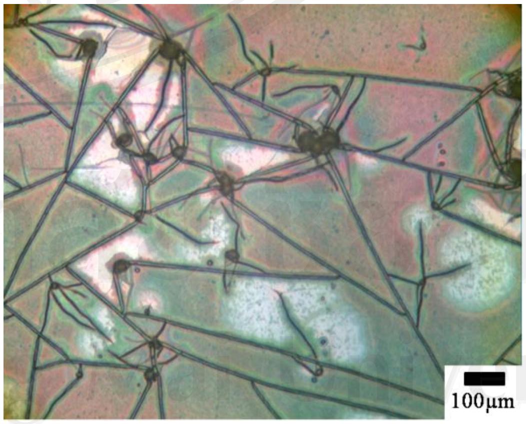

* 1) and 2) are heating condition for 1st and 2nd layers, respectively

Table 4.3 Optical micrographs of PZT/WO_3 nanocomposite thin films prepared with different processing conditions as shown in Table 3.3 (continue).

Condition	Film layer	Microstructure of films surface
7	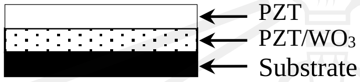 1) 400°C for 10 min 2) 400°C for 10 min then increased to 600°C with rate 6°C/min and leave for 30 min then cool down to room temperature; rate 10°C/min	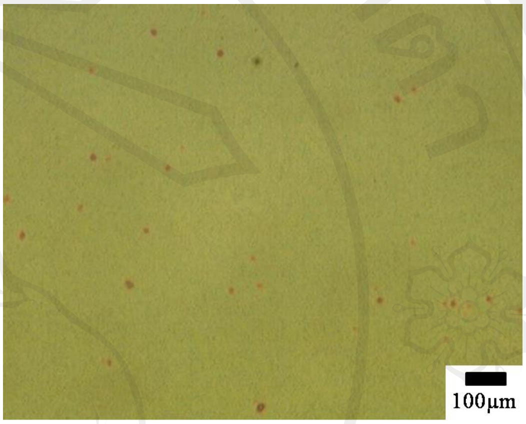
8	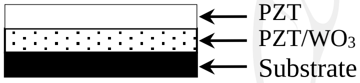 1) no heat 2) 400°C for 10 min then increased to 600°C with rate 6°C/min and leave for 30 min then cool down to room temperature; rate 10°C/min	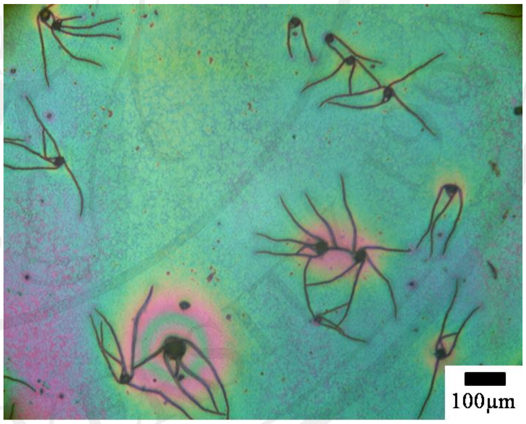

* 1) and 2) are heating condition for 1st and 2nd layers, respectively

Interestingly, the films had no crack when processed using the condition 7 (PZT/WO_3 film was pre-heated at 400°C for 10 min). Then a layer of PZT solution was subsequently deposited onto the PZT/WO_3 films. The sample was then heated on a hot-plate at 400°C for 10 min, and the heat was then gradually increased to 600°C using a rate of 6°C/min. After reaching 600°C, the heat was prolonged for 30 min and then cooled down to room temperature with a rate of 10°C/min. The above procedure explained an optimum condition that could reduce the thermal expansion mismatch of this film composite for a preparation of PZT-based nanocomposite thin films employed in this work.

When the microstructure of PZT composite film's surface was observed using SEM, a round curve-out was found near the crack (Fig. 4.9). This was believed to be a cluster of WO_3 nanoparticles under a thin surface as the energy dispersive x-ray spectra (EDS) detected a high ratio of tungsten at the curve area as shown in Fig. 4.9. Nevertheless, the flat surface of film in Fig. 4.10 was detected only PZT compositions for EDS analysis and the quantity of weight and atomic ratio of both area were shown in Table 4.4.

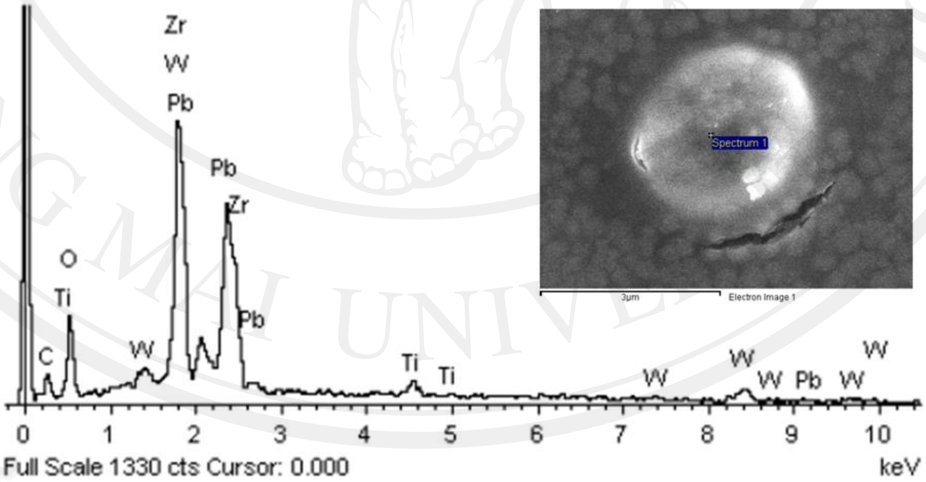

Figure 4.9 Energy dispersive x-ray spectra acuired from the round curve-out area.

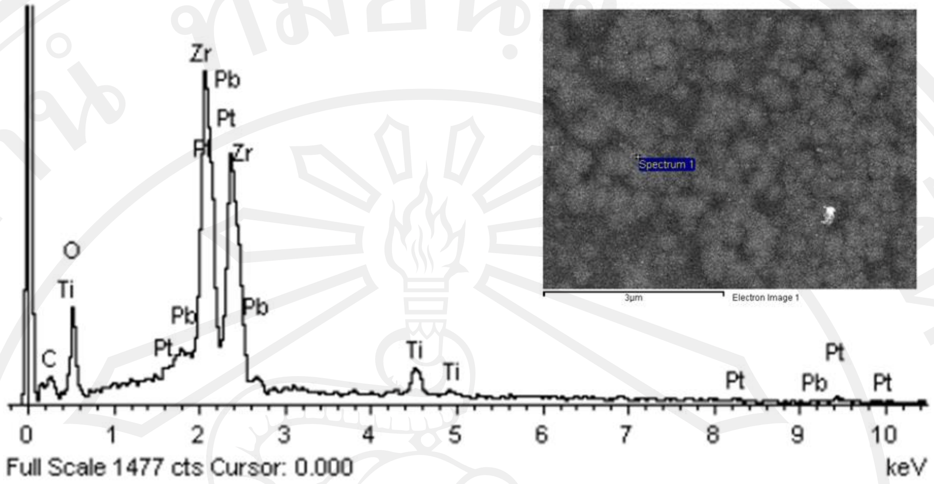

Figure 4.10 Energy dispersive x-ray spectra acuired from the flat area.

Table 4.4 The quantitative of weight and atomic ratio from EDS of both area.

Curve-out area			Flat smooth area		
Element	Weight%	Atomic%	Element	Weight%	Atomic%
C K	5.16	23.22	C K	4.12	19.16
O K	15.07	50.93	O K	14.72	51.34
Ti K	2.01	2.27	Ti K	4.13	4.81
Zr L	6.60	3.91	Zr L	10.18	6.23
W M	33.74	9.92	Pt M	27.02	7.73
Pb M	37.42	9.76	Pb M	39.84	10.73

4.2.2 Phase of PZT/WO_3 nanocompotie thin films

X-ray diffraction patterns with small angle technique of PZT/WO_3 nanocomposite thin films (condition 7) compared with the pure PZT thin films are shown in Fig. 4.11.

Both films were crystallized into perovskite phase with rhombohedral structure. In addition, the second phase (or pyrochlore phase) was not observed in both pure and composite films.

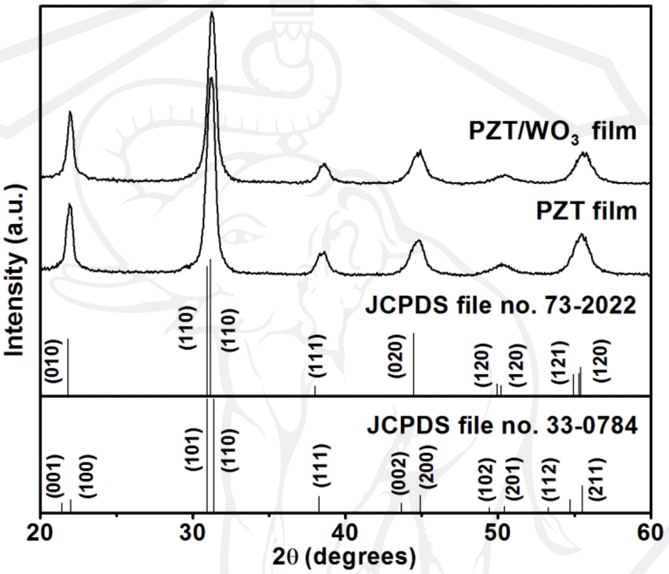

Figure 4.11 XRD patterns of PZT and PZT/WO_3 nanocomposite thin films

Considering the results of phase and microstructure, the heating condition 7 was found to be suitable for a preparation of PZT-based nanocomposite thin films for this work compared to the other conditions (the results given in Table 4.3). Therefore, two heating steps of the condition 7 was used to prepare both the PZT/WO_3 and PZT/CuO nanocomposite thin films for further study.

4.3 Conclusions of the optimized processing condition for preparation of PZT-based nanocomposite thin films

The PZT thin films were successfully fabricated using a triol sol-gel process. Annealing temperature and various amount of excess Pb affected phase and structure of the films. It was found that the crystalline perovskite phase of PZT started to be appeared at annealing temperature increased over 500°C. The fully crystallized perovskite phase of PZT without secondary phases was found in the film annealed at 600°C. When the annealing temperature was increased to 650°C, a pyrochlore phase appeared. Consequently, 600°C is the best annealing temperature for this work. In addition, the content of an excess Pb concentration was found to play an important role in the transformation from pyrochlore to perovskite as well as the nucleation and growth direction of the films. Furthermore, the increased Pb content promoted the dielectric properties of PZT thin films. The optimum Pb concentration for this work is 10 wt% due to the highest dielectric property.

Optimization for fabrication condition of the new nanocomposite PZT-based thin films was carried out by studying of the heating steps on microstructure of PZT-based nanocomposite films. The optimized processing condition for preparation of the PZT/WO_3 films consisted of two steps, i.e. (1) pre-heated the 1st layer PZT/WO_3 films at 400°C for 10 min and (2) infiltrated the defects with 2nd layer PZT film on the first layer, then annealed at 600°C for 30 min. With this procedure, the high quality composite film without crack could be achieved.

In further work, different types of nanoparticles will be added into PZT-based composite thin films. In this work, WO_3 and CuO nanoparticles were selected as a dispersed phases to investigate the effect of donor and acceptor dopants on electrical properties of the PZT film. The effects of lattice mismatch between PZT film and nanoparticles will be carefully observed and overcome by a hybrid process. The effects of type and quantity of the added-nanoparticles on phase, microstructure and electrical properties of the PZT thin film will be further investigated and discussed in details in the next chapters.